
Article:
Marcinkevics, R, O'Neill, J, Law, H et al. (2018) Multichannel electrocardiogram diagnostics for the diagnosis of arrhythmogenic right ventricular dysplasia. EP Europace, 20 (FI1). f13-f19. ISSN: 1099-5129

https://doi.org/10.1093/europace/eux124

Multichannel ECG diagnostics for the diagnosis of arrhythmogenic right ventricular dysplasia

Abstract

Background – The identification of arrhythmogenic right ventricular dysplasia (ARVD) from 12 channel standard ECG is challenging. High density ECG data may identify lead locations and criteria with a higher sensitivity.

Methods and Results – 80 channel ECG recording from patients diagnosed with ARVD and controls were quantified by magnitude and integral measures of QRS and T waves, and by a measure (the average silhouette width) of differences in the shapes of the normalised ECG cycles. The channels with the best separability between ARVD patients and controls were near the right ventricular wall, at the third intercostal space. These channels showed pronounced differences in P waves compared to controls, as well as the expected differences in QRS and T waves.

Conclusions – Multichannel recordings, as in body surface mapping, adds little to the reliability of diagnosing ARVD from ECGs. However, repositioning ECG electrodes to a high anterior position can improve the identification of ECG variations in ARVD. Additionally, increased P wave amplitude appears to be associated with ARVD.

Key words:

Arrhythmogenic cardiomyopathy

Arrhythmogenic right ventricular cardiomyopathy

Arrhythmogenic right ventricular dysplasia

Multichannel ECG recording

P wave amplitude

Multichannel ECG diagnostics for the diagnosis of arrhythmogenic right ventricular dysplasia

Condensed abstract

This study examines the use of 80-lead ECGs in the diagnosis of arrhythmogenic right ventricular dysplasia (ARVD). Findings show that high anterior chest lead positions improve diagnosis of ARVD and interestingly, ARVD patients have increased P-wave amplitude. However, additional channels of 80-lead ECGs add little in the diagnosis of ARVD.

Multichannel ECG diagnostics for the diagnosis of Arrhythmogenic Right Ventricular Dysplasia

Ricards Marcinkevics[1], James O'Neill[2] MB BS, Hannah Law[2] BSc, Eleftheria Pervolaraki[3] PhD, Andrew Hogarth[2] MB ChB, PhD; Craig Russell[2] MSc, Berthold Stegemann[1] PhD , Arun V. Holden[3] PhD , Muzahir H Tayebjee[2] MD

[1]*Medtronic Plc, Bakken Research Center, 11 Maastricht, The Netherlands*

[2] *West Yorkshire Arrhythmia Service, Leeds General Infirmary, Great George Street, Leeds, LS1 3EX, UK*

[3]*School of Biomedical Sciences, University of Leeds, Leeds, LS2 9JT; UK*

Corresponding author:

Dr MH Tayebjee

West Yorkshire Arrhythmia Service, Leeds General Infirmary, Great George Street, Leeds, LS1 3EX, UK. Tel: 0113 392 6619. Fax: 0113 392 3981. E-mail: muzahir.tayebjee@nhs.net

Total word count: 3,049 words

Journal Subject Terms: Arrhythmia, Electrocardiogram (ECG)

What's New?

- 80 channel ECG recordings from ARVD patient and control groups allow the selection of recording sites that are best for separating the ECG waveforms between the two groups, using methods based on the ECG waveform rather than measures of amplitudes and durations of its components.
- These methods show that high anterior chest lead positions provide the most discrimination between ARVD patients and controls and demonstrate well-known differences in T wave polarity and QRS integral.
- There is also an association between increased P wave amplitude and the presence of ARVD.
- The additional channels of the 80-lead ECGs add little to the discriminability between ARVD patients and controls.

Introduction

The 2010 Task force criteria for the diagnosis of arrhythmogenic right ventricular dysplasia (ARVD) include multiple 12 lead electrocardiographic (ECG) criteria[1]. These contribute both major (T wave inversion (TWI)) in right sided precordial, V1-V3, or beyond in the absence of right bundle branch block (RBBB), epsilon wave and minor (TWI in V1 and V2 in the absence of RBBB or in V4-V6, TWI in V1-V4 in presence of RBBB, terminal activation of the QRS 55ms in the absence of complete RBBB) diagnostic criteria. These ECG criteria mostly relate to the spread of repolarization. Changes in repolarizaton can appear earlier in the disease progression and provide a specific finding[2]. Analysis of the 12 lead ECG for dispersion of depolarization (QRS) and depolarization-repolarization (QT) intervals across the precordial leads can lend added information in risk stratification of individuals already diagnosed with ARVD[3].

The analysis of the ECG for ARVD diagnosis is principally based upon standard 12 lead ECG data. However, it is not known whether ECG diagnosis may be improved with high density body surface ECG mapping or by leads in nonstandard locations. The 12 lead ECG has inherent limitations. The density of ECG mapping of the right ventricle is limited, and the ability to compare electrical activity between the left and the right precordium restricted. High density body surface mapping with an 80 lead ECG has previously been shown to improve the sensitivity of diagnosis of acute myocardial infarction[4], particularly with improvements in posterior and inferior wall infarction recognition; anatomical areas accepted to be relatively sparsely represented with conventional 12 lead ECG mapping. Published data regarding high density ECG mapping in ARVD is limited, with focus on the differentiation between ARVD and normal heart right ventricular outflow tract tachycardia (RVOT) with regard to T-wave characteristics only[5].

The present study was therefore planned to determine whether a commercially available 80 lead surface ECG would lead to a characterization of depolarization and repolarization across the chest leads in patients with ARVD which could then identify ECG lead locations and criteria with higher sensitivity.

Methods

Recruitment

Nine unrelated ARVD patients, who had given written informed consent to participate in this electrophysiological study, were recruited from the West Yorkshire Arrhythmia Service Outpatient Clinic during a six month period in 2013. An equal number of controls of similar age and gender as well as body size were recruited from hospital and university staff. All control subjects had a normal echocardiogram. The study protocol received approval from the NHS Health Research Authority NRES Committee Yorkshire & The Humber.

Diagnosis of ARVD

The patients had been diagnosed with ARVD on the basis of the 2010 modified criteria which updates the 1994 guidelines[1, 6].

Evaluation and Clinical Testing

The patients' medical history was obtained from review of their records and by interview, and is summarized in Tables 1 and 2.

Body surface ECGs, with the subject resting and supine, were recorded by an 80-lead system from Verathon (Bothell, Washington) Heartscape® with 58 anterior, 12 lateral and 10

posterior leads - see Figure 1(a). Electrode contact was automatically checked when the electrode vest was applied, and heart rate, QRS width, QT,QTc and QRS axis/T axis, sample ECGs for each channel, and a standard "12 lead ECG" reconstructed from the 80 channels printed after a 10s recording. A ten second 80 channel ECG recording at a sampling rate of 1ms was stored. Channels with poor electrode contact identified by excessive noise on the lead were excluded from the analysis

Independent Data Analysis

The stored data was exported, converted from a proprietary .hs format to a .csv format by a MatLab program, for plotting and processing. For each recording, the activity of each channel was quantified by the following measures: magnitude (peak-to-peak), and sum (positive peak value + negative peak), and the integrals of the depolarization (QRS) and repolarization (T) wave components.

In order to quantify the similarity of signals in patients and controls for each channel the duration of each cycle of the ECG was normalised to eliminate the effects of heart rate. A dynamic time warping distance measurement was used to quantify the dis-similarity between any two signals. Technical details are given in the Appendix A. The compactness (see supplementary material A.1) of the patient and control clusters were measured, and the separation (see supplementary material A.2) between them, to determine which channels i.e. electrode positions gave the clearer separation between ARVD patients and controls. The separability was quantified by the average silhouette width as defined in Supplementary material A.3.

The data analysis protocol is illustrated schematically in figure 1.

Results

There were no differences in baseline characteristics between ARVD patients and controls (Table 1) apart from a lower heart rate in ARVD patients due to beta-blocker use. All patients had clear task force criteria for ARVD (Table 2).

Scatter plots for all 80 channels of integrals magnitudes and signed amplitudes for QRS and T wave showed no clear visual separation between ARVD and control data apart from the polarity of the T waves in the anterior chest leads. Figure 2a is an example of this illustrated for the signed T wave amplitude and QRS integral for leads placed in a similar anatomical location as leads V1 to V6 on a standard 12 lead ECG. Figure 2b shows the same for leads that were placed to cover the anterior aspect of the right ventricle.

Average silhouette width (ASW) is a measure of the separability between ARVD and controls for an individual channel, and indicates the diagnostic usefulness of the channel. The ASW was calculated for every ECG channel 1-77, and is shown in Figure 3. Their value was colour coded and their location indicated by superposition over an image of the torso. The channels with the largest ASW *i.e.* the most compact and the most clearly separable clusters for the ECG time series of ARVD patients and normal subjects was channel 21, which was 3 cms above V_1 (3rd intercostal space to the right of the sternum) . Most of the channels with greater ASWs were located close to and around channel 21 (30, 31, 32, 33 and 34) *i.e.* near the anterior right ventricular wall. Channel positions with less separable clusters of time series were also topographically close to each other.

In order to visualise the characteristics of the waveform that were different between patients with ARVD and controls, the ten second recording was normalised for amplitude (Figure 4).

The channels with high ASW (with greater separability measure values) demonstrated clear differences between ARVD patients and controls. In the ARVD patients the T wave polarity was more often negative and the S wave of the QRS was more delayed and pronounced as expected. Interestingly however, the visualised P wave was larger in amplitude. This can be quantified by the half integral of the P wave (time from peak to end of wave) , which fo the channels a,b,c, of Fig 4 was 0.019 ±0.015 for patients, 0.007± 0.005, P= 0.0007, mean±standard deviation .

To ensure that the evaluation of channels which were based upon the ASW measure were plausible as a diagnostic index, subjects were classified using multiple channels[7]. We anticipated that recordings from channels with greater ASWs would be more effective in the classification of subjects. Using a simulated annealing algorithm, a set of channels, as well as weights for them, were tuned for the 1NN classifier, only allowing channels with greater ASW values to be selected. 1NN algorithm based using the channels C=(20,21,23,31,41) and with weights w= (0.700,0.630,0.015,0.091,0.523) achieved an accuracy of 81.3%.

In order to provide statistical evidence that the performance of this algorithm was not a coincidence, the accuracies of 1000 1NN classifiers based on sets of randomly chosen channels with randomly assigned weights were measured, using leave-one-out procedure. The nearest neighbour algorithm using the ECG channels that had been selected on the basis of their average silhouette widths provided the greatest accuracy, confirming the suitability of the ASW measure to select channels for the ECG classification

Discussion

ARVD is an inherited condition in which the myocardium gradually undergoes fibrofatty replacement over time[8]. As its name suggests, it was initially felt to be a disease of the right ventricle but there is now evidence of left ventricular and bi-ventricular forms[9-11]. Those affected are often asymptomatic and the first manifestation can be with a sudden, unexplained death. Although standard 12-lead ECGs, signal-averaged ECGs and cardiac MRI may show abnormalities, these changes generally occur once the disease is well established and so diagnosis of the condition remains a challenge. This is the first report in which multi-electrode surface ECG mapping was used to determine whether the addition of multiple leads increases the sensitivity of diagnosis.

The multichannel ECG leads are analysed in terms of their complete waveform shapes, rather than simple measures of amplitudes, intervals and durations. A dynamic time-warping distance measure is used to quantify the differences between the ECG waveform shapes between the ARVD patients and controls, and the separability measured to determine which recording positions give the clearest separation between the ARVD patients and control groups.

Our results show that the high anterior chest leads provide the most discrimination between ARVD patients and controls with differences in T wave polarity and QRS integral. It is not surprising that the channels adjacent to the anterior right ventricle are more discriminatory than the other ECG leads since the condition generally manifests with right ventricular pathology. This lead position is also in a similar location to the previously described Fontaine lead position[11, 12].

A more unexpected finding is the enhanced P wave amplitude in ARVD patients in these electrode positions. The morphology of the P wave is more consistent with right atrial pathology due to the increased P wave amplitude and suggests either a right atrial cardiomyopathic process or right atrial remodelling. This would be in keeping with previous studies which have demonstrated an increased prevalence of atrial arrhythmias and structural variations in patients with ARVD[11, 13-17]. However, further evaluation of this finding is required to determine its use in the diagnosis of ARVD.

The majority of the channels did not provide additional discriminatory information and so high-density ECG recording does not appear to be necessary. Instead, simply repositioning standard ECG electrodes to a higher anterior position may be all that is required to support the clinical diagnosis of ARVD.

Limitations

This is a small single centre study, however ARVD is a rare condition and our results would need to be tested in a larger multicentre population. Further, we chose patients with a definitive diagnosis, and testing these criteria in patients with phenotypically less severe disease would be useful. Our Controls were identified on the basis of a normal ECG and echocardiogram. Ideally, controls would also have a cardiac MRI to exclude quiescent forms of ARVD but this pilot study was not resourced to enable this.

Conclusion

In patients with confirmed ARVD, the high anterior chest leads appear to be better at discriminating the changes in QRS integral and T wave polarity between patients and controls. Furthermore, there appears to be an association between increased P wave

amplitude and the presence of ARVD. These findings therefore suggest that the addition of high anterior leads and P wave amplitude as part of the diagnostic work up of ARVD may improve the diagnostic yield. The additional channels that can be measured with 80-lead ECGs are not useful and clinically it may be more practical and economical to place electrodes in these areas.

Acknowledgments

We would like to thank Fuxing Yang, Jong Tae Yuk, Matthew Caprio, Keith Coomes and Julie Lyon from Verathon for the support they provided during the study, their loan of equipment and assistance with data decoding. We would also like to thank Christopher Whitaker for his assistance with data processing.

Funding Sources

Verathon provided equipment and assisted in the initial processing of raw data.

Disclosures

James O'Neill has received a fellowship from St. Jude Medical. Andrew Hogarth has received travel grants from St. Jude Medical. Muzahir Tayebjee has received research/travel grants from St. Jude Medical, Biosense Webster, Medtronic and Boehringer Ingelheim.

References

1. Marcus FI, McKenna WJ, Sherrill D, Basso C, Bauce B, Bluemke DA, et al. Diagnosis of arrhythmogenic right ventricular cardiomyopathy/dysplasia: Proposed modification of the task force criteria. *Eur Heart J*. 2010;31:806-814

2. Marcus FI. Prevalence of t-wave inversion beyond v1 in young normal individuals and usefulness for the diagnosis of arrhythmogenic right ventricular cardiomyopathy/dysplasia. *Am J Cardiol*. 2005;95:1070-1071

3. Turrini P, Corrado D, Basso C, Nava A, Bauce B, Thiene G. Dispersion of ventricular depolarization-repolarization: A noninvasive marker for risk stratification in arrhythmogenic right ventricular cardiomyopathy. *Circulation*. 2001;103:3075-3080

4. McClelland AJ, Owens CG, Menown IB, Lown M, Adgey AA. Comparison of the 80-lead body surface map to physician and to 12-lead electrocardiogram in detection of acute myocardial infarction. *Am J Cardiol*. 2003;92:252-257

5. Samol A, Wollmann C, Vahlhaus C, Gerss J, Bruns HJ, Breithardt G, et al. T-wave integral: An electrocardiographic marker discriminating patients with arrhythmogenic right ventricular cardiomyopathy from patients with right ventricular outflow tract tachycardia. *Europace*. 2013;15:582-589

6. Marcus FI, McKenna WJ, Sherrill D, Basso C, Bauce B, Bluemke DA, et al. Diagnosis of arrhythmogenic right ventricular cardiomyopathy/dysplasia: Proposed modification of the task force criteria. *Circulation*. 2010;121:1533-1541

7. Mitchell TM. *Machine learning*. New York: McGraw-Hill; 1997.

8. Hauer RN. Arrhythmogenic right ventricular dysplasia/cardiomyopathy: Arrhythmogenesis in the apparently normal heart? *Europace*. 2016;18:953-954

9. Berte B, Denis A, Amraoui S, Yamashita S, Komatsu Y, Pillois X, et al. Characterization of the left-sided substrate in arrhythmogenic right ventricular cardiomyopathy. *Circ Arrhythm Electrophysiol*. 2015;8:1403-1412

10. Coats CJ, Quarta G, Flett AS, Pantazis AA, McKenna WJ, Moon JC. Arrhythmogenic left ventricular cardiomyopathy. *Circulation*. 2009;120:2613-2614

11. Fontaine GH, Duthoit G, Li G, Andreoletti L, Gandjbakhch E, Frank R. Epsilon wave on an electronic loop in a case of arrhythmogenic right ventricular dysplasia with myocarditis: An updated definition of the epsilon wave. *Europace*. 2017. Epub ahead of print. 10.1093/europace/euw320

12. Hurst JW. Naming of the waves in the ecg, with a brief account of their genesis. *Circulation*. 1998;98:1937-1942

13. Tonet JL, Castro-Miranda R, Iwa T, Poulain F, Frank R, Fontaine GH. Frequency of supraventricular tachyarrhythmias in arrhythmogenic right ventricular dysplasia. *Am J Cardiol*. 1991;67:1153

14. Brembilla-Perrot B, Jacquemin L, Houplon P, Houriez P, Beurrier D, Berder V, et al. Increased atrial vulnerability in arrhythmogenic right ventricular disease. *Am Heart J*. 1998;135:748-754

15. Chu AF, Zado E, Marchlinski FE. Atrial arrhythmias in patients with arrhythmogenic right ventricular cardiomyopathy/dysplasia and ventricular tachycardia. *Am J Cardiol*. 2010;106:720-722

16. Camm CF, James CA, Tichnell C, Murray B, Bhonsale A, te Riele AS, et al. Prevalence of atrial arrhythmias in arrhythmogenic right ventricular dysplasia/cardiomyopathy. *Heart Rhythm*. 2013;10:1661-1668

17. Saguner AM, Vecchiati A, Baldinger SH, Rueger S, Medeiros-Domingo A, Mueller-Burri AS, et al. Different prognostic value of functional right ventricular parameters in arrhythmogenic right ventricular cardiomyopathy/dysplasia. *Circulation. Cardiovascular imaging*. 2014;7:230-239

Table 1 Baseline Characteristics

	Controls (n=10)	Patients (n=9)	P
Age (years)	50±15	54±14	0.563
Male (%)	80	80	1.00
Height (m)	1.73±0.09	1.79±0.10	0.163
Weight (kg)	79±15	86±14	0.295
BMI (kg/m^2)	26±3	27±4	0.753
Heart rate (b/min)	70±8	58±10	0.009
PR (ms)	161±14	181±67	0.376
QRS duration (ms)	91±11	98±19	0.369
QT interval	415±19	429±27	0.258

Table 2. Clinical characteristics of ARVD patients

Study no.	Global or regional dysfunction and structural alterations			Repolarisation abnormalities		Depolarisation/ conduction abnormalities		Arrhythmias		Family history		Exact details
	MRI		RV angio									
	Major	Minor	Major	Major	Minor	Major	Minor	Major	Minor	Major	Minor	
ACP001			1		1	1						Repol: (2012) - TWI in V1+V2, Depol: (2006) - epsilon wave in V1-V3 on ECG in Newcastle with Dr Furniss, RV angio: (2006) - RV dysplasia
ACP002	1				1				1			MRI: (2007) - Akinesis, EF<40%.Repol abn: (2007) - T wave inv V1+V2, Arrhyth:(1997) >500VEs on 24tape
ACP003	1					1			1			MRI: (2002) - RV dyskinesia + RVEF<40%.Depolar: (2009) - epsilon wave in V1-V3. Arrhyth: (2002) - VT with LBBB and inf axis,
ACP004		1			1	1			1			MRI: (2011) - report states 'meets minor criteria for taskforce'.Depol (2011) - epsilon wave in V1-V3. Arrhyth: (2011) - VT with LBB and inf axis, Repol: (2011) - TWI V1+V2
ACP005	1					1						MRI (2007) - abnormal fatty deposits, RWMA, Depol (2007) - epsilon wave in V1-V3
ACP006			1							1		RV angio (2000) - 'dilated, abnormally contracting RV'. Positive gene test for ARVD.
ACP007	1				1			1			1	MRI: (2002) - RV dysplasia + EF<40% Arrhyth:(2002) Sustained VT with LBBB with superior axis, Repol: (2003) - TWI in V1+V2. Family Hx (2002) - sudden death of father (no ARVD Dx)
ACP008	1				1				2			MRI: (2000) - RV regional dyskenesia, fatty deposits, RVEDV 194.9ml, RVESV 109.6ml, RV stoke vol 83.2ml, RV EF <40%. Repol abnormalities:(2000) T wave inv V1+V2 (no RBBB), Arrhyth: (1997+1999)>500VEs on 24hr tape, (1997) VT on EP study - LBBB with inf axis
ACP009		1			1			1				Arrhyth:Sustained VT with LBBB with superior axis, Repol abn:TWI V1+V2(2009), MRI:(2008) RV akinesia + RVEDV/BSA=100ml/m2

Figure 1 Data analysis protocol

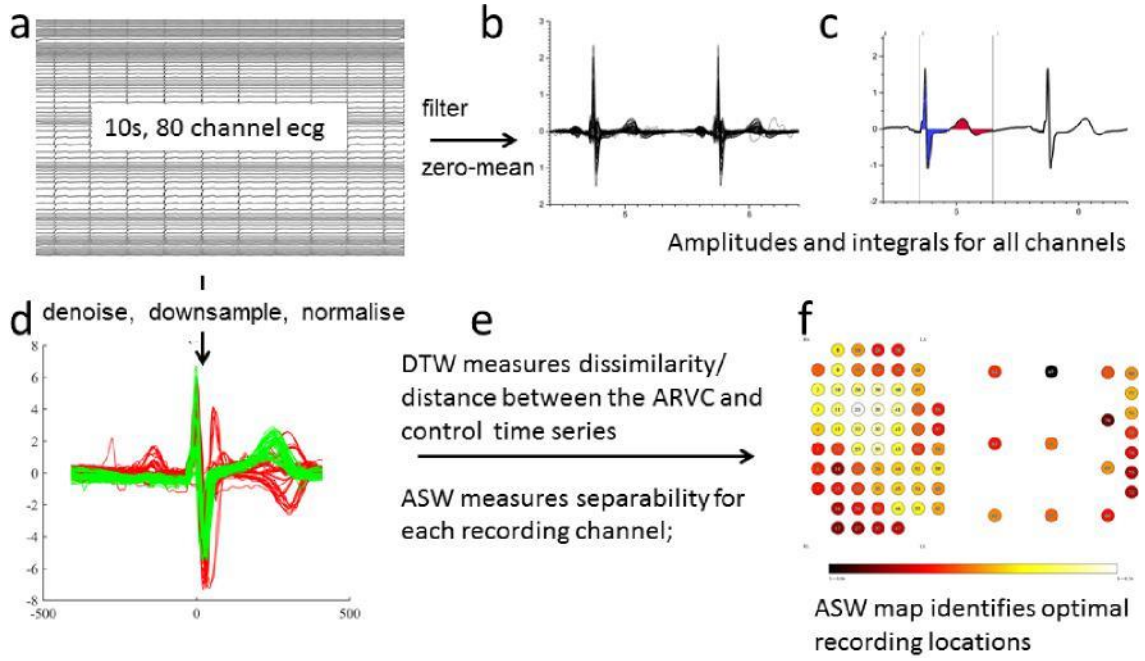

(a) 80 channels, 10s, recorded at 1kHz. ***(b)*** Each channel is zero-meaned and filtered, and the ***(c)*** amplitudes and integrals of the QRS (blue) and T wave (red) components obtained algorithmically for each channel; ***(d)*** each channel is denoised, downsampled and normalised, ***(e)*** for each channel the dynamic time warping DTW distance to all the other same channels in both patients and controls, for the average cycle, is estimated. ***(f)*** The separability of each channel (i.e. how well it can separate ARVD patient and control groups) is measured and mapped by the average silhouette width (ASW). Further details can be found in the supplementary material.

Figure 2 Overlap of ECG measures between patients and controls.

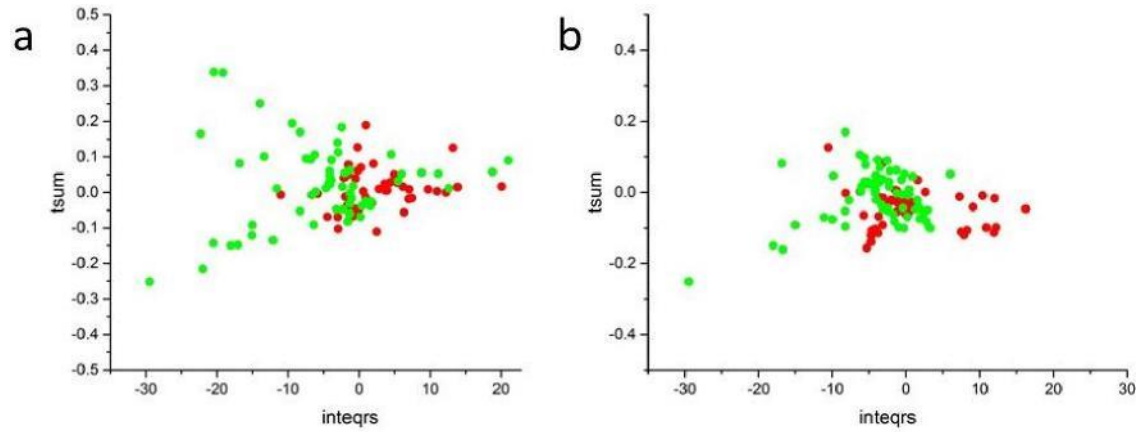

Signed amplitude of T wave and integral of QRS for all ARVD patients (red) and controls (green). ***Figure a*** shows electrode positions corresponding to V1 to V6 on a standard 12 lead ECG and ***figure b*** shows electrodes positioned over an area covering the anterior aspect of the right ventricle.

Figure 3 Electrode positions on (a) anterior and (b) posterior torso.

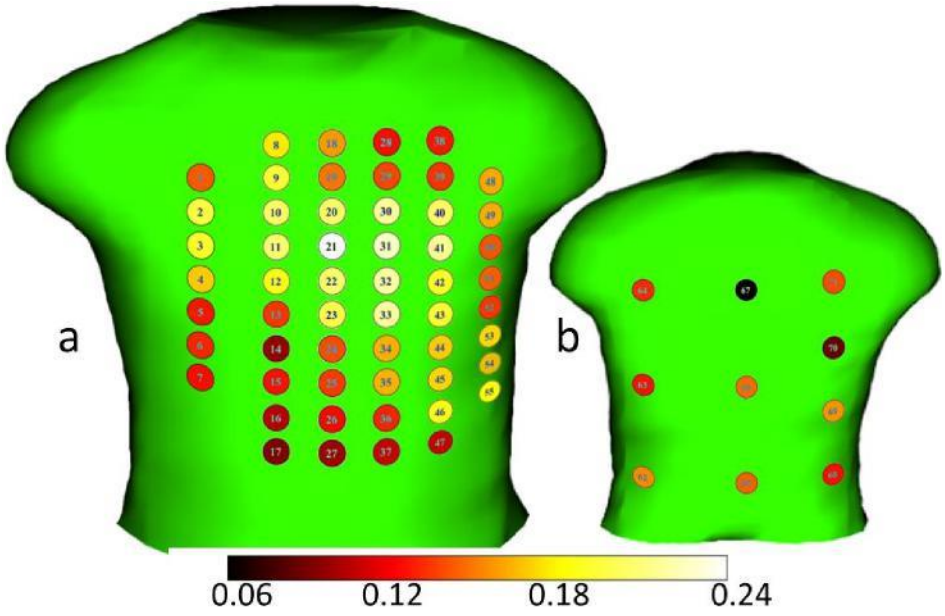

Colour map (hot metal scale) codes electrodes which discriminate between ARVD and control recordings. White represents best separation, dark red is least useful in discriminating between ARVD and controls. The numbers refer to the recording channel, and the colour codes the Average Silhouette Width calculated from equation A.3 (see Supplmentary Material).

Figure 4 Ten seconds of superimposed normalised cycles of ECGs for single recording channels for ARVD patients (red) and controls (green), centred at the peak of the R wave

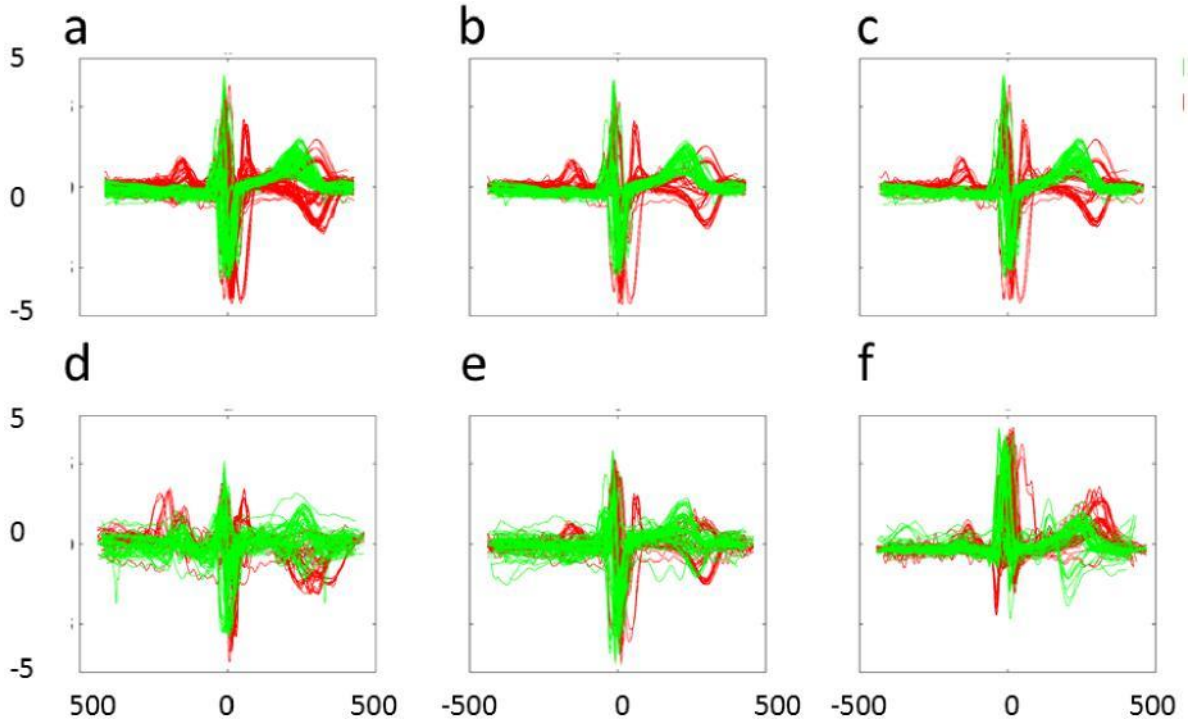

The amplitude for each channel of the 10s was zero-meaned, de-noised and normalised by its standard deviation. ***a,b,c*** are channels 21,31 and 32, the three channels with the highest value of ASW (ASW > 0.3). ***d,e,f*** are channels 14,29 and 26 with ASW < 0.15.

Appendix A.

The ECG recording from any single channel in one person can be represented as discrete time series $T = [p_1, p_2, \dots, p_{n-1}, p_n]$, where every point p_i is a value of the ECG signal in that channel (note that the time stamps of points are omitted, because all of the signals were acquired at the same sampling rate) [8]. Based on this formal representation of ECG data as n-dimensional vectors, we can define a distance function $d(T_1, T_2)$ quantifying the dissimilarity between two time series T_1 and T_2. A straightforward and commonly used measure is the Euclidean distance [8], however, in our analysis the dynamic time warping (DTW) distance was applied [9], in order to be able to address the problem of variation in the ~~speed~~ period of time series/heart rates between recordings from subjects..

Given the distances between time series in every channel, the compactness and separation of the clusters of ARVC patients and normal subjects can be evaluated by the average silhouette width as defined in [10]. Here we use the silhouette to quantify the separability of two classes.

For every channel, let $\mathbb{T}_A$ denote a set of ARVC patient time series and $\mathbb{T}_N$ denote a set of control subject time series. For every subject i, let $a(i)$ be the average distance of the time series of subject i to the time series of the subjects in the same class

$$a(i) = \mathbf{1}_{\mathbb{T}_A}(T_i) \sum_{T_j \in \mathbb{T}_A} \frac{d(T_i,T_j)}{|\mathbb{T}_A|} + \mathbf{1}_{\mathbb{T}_N}(T_i) \sum_{T_j \in \mathbb{T}_N} \frac{d(T_i,T_j)}{|\mathbb{T}_N|}, \quad \text{(A 1)}$$

where $\mathbf{1}_X(\cdot)$ is an indicator function for set X. Let $b(i)$ denote the average distance of the time series of subject i to the time series of subjects in the opposite class

$$b(i) = \mathbf{1}_{\mathbb{T}_A}(T_i) \sum_{T_j \in \mathbb{T}_N} \frac{d(T_i,T_j)}{|\mathbb{T}_N|} + \mathbf{1}_{\mathbb{T}_N}(T_i) \sum_{T_j \in \mathbb{T}_A} \frac{d(T_i,T_j)}{|\mathbb{T}_A|}. \quad \text{(A 2)}$$

Finally, number $s(i)$ [10] for every time series can be defined as

$$s(i) = \frac{b(i) - a(i)}{\max\{a(i), b(i)\}}.$$

Once values $s(i)$ are computed for every time series in $\mathbb{T}_A$ and $\mathbb{T}_N$, the average silhouette width (ASW) S_c can be used as a measure of class separability for every channel c

$$S_c = \frac{1}{|\mathbb{T}_A| + |\mathbb{T}_N|} \sum_i s(i). \quad \text{(A 3)}$$

The greater the value of S_c for channel c, the more separable and the tighter are the clusters formed by the time series of ARVC patients and the series of control subjects for the channel. This measure can be useful in identifying which channels are better suited for diagnosis of ARVC.

Calculations were in the MATLAB numerical computing environment, raw ECG time series were de-noised using the wden automatic de-noising function based on wavelets (db4

wavelet, level 4). De-noised time series were down-sampled from 1000 Hz to 100 Hz. Measure values for every channel were then calculated

Furthermore, the performance of channels with greater ASWs was evaluated using the k-Nearest Neighbor (k-NN) classification algorithm [11], in particular, using 1NN. The accuracy of the 1NN classifier based on the set of channels with greater ASW values was compared to the accuracies of nearest neighbor classifiers defined on sets of randomly selected channels. The 1NN classifier was chosen, because it is straightforwardly implementable and, therefore, the results can be easily reproduced. The summary of the 1NN classification algorithm for multi-channel ECG time series is provided as pseudocode in Algorithm 1. As can be seen, this algorithm uses a weighted sum of distances in chosen ECG channels; this similarity measure allows for classification based on multiple channels in conjunction.

- **Algorithm 1** Multi-channel ECG Time Series Classification with 1NN Algorithm

---

- **Input**: Labelled time series data sets for every channel, where $T_{i,j}$ refers to the time $C = (i_1, i_2, \dots, i_m)$ to be used in classification; list of weights $W = (w_1, w_2, \dots, w_m)$, where w_j is the weight for the channel with index i_j; unlabelled time series data sets for every channel for an unclassified subject x
- **Output**: Class label for subject x
- \\ weighted sum of distances in multiple channels
- 1: Let s be a subject with minimal $\sum_{j=1}^{m} w_j d(T_{j,s}, T_{j,x})$
- 2: **return** Class label of s
